

# Tricritical behavior and magnetic properties for a mixed spin-1 and spin- $\frac{3}{2}$ transverse Ising model with a crystal field

Wei Jiang\*

Shenyang National Laboratory for Materials Science, Institute of Metal Research, Chinese Academy of Sciences,  
Shenyang 110016, People's Republic of China  
and College of Sciences, Shenyang University of Technology, Shenyang 110023, People's Republic of China

Guo-zhu Wei

College of Sciences, Northeastern University, Shenyang 110006, People's Republic of China

Zhi-dong Zhang

Shenyang National Laboratory for Materials Science, Institute of Metal Research, Chinese Academy of Sciences,  
Shenyang 110016, People's Republic of China  
and International Centre for Material Physics, Chinese Academy of Sciences, Shenyang 110016, People's Republic of China

(Received 16 April 2002; revised manuscript received 11 June 2003; published 20 October 2003)

An effective-field theory is developed for a mixed Ising system, consisting of spin 1 and spin  $\frac{3}{2}$  with different anisotropies in a transverse field on a honeycomb ( $z=3$ ) lattice. The general formula for determining the phase diagram of transition temperatures and tricritical points is derived and the temperature dependence of the total magnetization of the system is calculated. Some interesting phenomena, such as the appearance of two tricritical points and the existence of two compensation points in a ferrimagnet, are found and the physics beyond these phenomena are discussed in detail. The competition among the exchange coupling, the anisotropies, the transverse field, and the temperature has a profound effect on the characteristic of magnetic phases in the mixed-spin systems.

DOI: 10.1103/PhysRevB.68.134432

PACS number(s): 75.10.Hk, 75.30.Gw, 75.10.Dg, 75.50.Gg

## I. INTRODUCTION

Mixed-spin Ising systems provide simple but interesting models to study molecular magnetic materials that are considered to be possibly useful materials for magneto-optical recording.<sup>1-3</sup> The investigation of ferrimagnetism in these systems has rapidly become a very active research field, which is very important from the point of view of either fundamental research or technologies, since the ferrimagnetic order plays an important role in these materials. Most of these studies treated the mixed-spin Ising systems with spin  $\frac{1}{2}$  and spin  $S$  ( $S > \frac{1}{2}$ ) in a uniaxial crystal field or a transverse field. The systems have been discussed by the use of the exact method,<sup>4</sup> the Monte Carlo simulation,<sup>5-7</sup> the effective-field theory (EFT),<sup>8-12</sup> the high-temperature series expansion method,<sup>13,14</sup> the method of combining the pair approximation with the discretized path integral representation,<sup>15</sup> and the renormalization-group technique.<sup>16</sup>

Recently, attention has been directed to mixed-spin systems where both constituents have spin values larger than  $\frac{1}{2}$ .<sup>17,18</sup> Various types of magnetic anisotropies have a profound effect on the characteristic of magnetic phases in the spin systems. An example is the anisotropy due to the crystal field, which affects the symmetries of the magnetic systems. In our recent paper,<sup>19</sup> the EFT was applied to the mixed spin- $\frac{1}{2}$  and spin- $\frac{3}{2}$  transverse Ising model, in which a single-ion anisotropy was considered. It was found that the tricritical behavior does not exist in that system. The EFT method, without introducing mathematical complexities, can include some effects of spin-spin correlations and provide results that are quite superior to those obtained by a normal

mean-field theory. It has been applied successfully to various physical problems. As far as we know, however, the properties of the mixed spin-1 and spin- $\frac{3}{2}$  transverse Ising model with different single-ion anisotropies have not been examined in detail, owing to the difficulty that the eigenvalues of the Hamiltonian in this system cannot be given analytically. The purpose of this work is to find out whether there are tricritical points in the mixed spin-1 and spin- $\frac{3}{2}$  transverse Ising model with different crystal fields for a honeycomb lattice. The magnetic properties of the present systems are studied systematically. Some interesting phenomena, such as the appearance of two tricritical points and the existence of two compensation points in a ferrimagnet, are found.

The paper is organized as follows. In Sec. II, we introduce briefly the basic framework of the EFT theory<sup>19,20</sup> and give the formulation for the mixed spin-1 and spin- $\frac{3}{2}$  transverse Ising model with different crystal fields for the honeycomb lattice. In Sec. III, the numerical results for the phase diagrams and the magnetization are studied in detail. Finally, we give the summary in Sec. IV.

## II. FORMULATIONS

The Hamiltonian of the mixed spin-1 and spin- $\frac{3}{2}$  Ising model is given by

$$H = -J \sum_{\langle i,j \rangle} \sigma_i^z \sigma_j^z - \Omega \sum_i \sigma_i^x - \Omega \sum_j S_j^x - D_A \sum_i (\sigma_i^z)^2 - D_B \sum_j (S_j^z)^2, \quad (1)$$

with spin 1 and spin moments  $\sigma_i^z$  and  $\sigma_i^x$  at site  $i$  in sublattice  $A$ , spin  $\frac{3}{2}$  and spin moments  $S_j^z$  and  $S_j^x$  at site  $j$  in sublattice  $B$ , and where the first summation is carried out only over nearest-neighbor pairs of spins.  $J$  is the exchange interaction constant, and  $D_A$  and  $D_B$  are the crystal field interactions that come from the sublattices  $A$  and  $B$ , respectively.  $\Omega$  represents the transverse field.

The starting point for the statistics of our spin system for any operator  $A_i$  at site  $i$  is given by<sup>21</sup>

$$\langle A_i \rangle = \left\langle \frac{\text{Tr}_{(i)} A_i \exp(-\beta H_i)}{\text{Tr}_{(i)} \exp(-\beta H_i)} \right\rangle, \quad \beta = 1/k_B T \quad (2)$$

where  $T$  is the absolute temperature and  $k_B$  is Boltzmann constant.  $\text{Tr}_{(i)}$  denotes a partial trace for the site  $i$ .  $\langle \cdots \rangle$  denotes the canonical ensemble average. For the derivation, let us separate the Hamiltonian (1) into two parts:<sup>22</sup> one (denoted by  $H_i$ ) includes all contributions associated with the site  $i$ , and the other (denoted by  $H'_i$ ) does not depend on the site  $i$ . Then, we rewrite the Hamiltonian at site  $i$  in the sublattice  $A$  in the following form:

$$\begin{aligned} H &= -J \sum_j S_j^z \sigma_i^z - J \sum_{i'j} \sigma_{i'}^z S_j^z - D_A (\sigma_i^z)^2 - D_A \sum_{i'} (\sigma_{i'}^z)^2 \\ &\quad - \Omega \sigma_i^x - \Omega \sum_{i'} \sigma_{i'}^x - D_B \sum_j (S_j^z)^2 - \Omega \sum_j S_j^x \\ &= H_i + H'_i \quad (i \neq i'), \end{aligned} \quad (3)$$

where

$$-H_i = E_i \sigma_i^z + D_A (\sigma_i^z)^2 + \Omega \sigma_i^x \quad (4)$$

and

$$E_i = J \sum_j S_j^z, \quad (5)$$

where  $E_i$  is the operator expressing the local field on the site  $i$ . Owing to the term of including the transverse field ( $\Omega \sigma_i^x$ ) in Hamiltonian  $H_i$ , the terms  $H_i$  and  $H'_i$  do not commute with each other. In the  $\sigma^2$ ,  $\sigma_z$  representation, the diagonalization of  $-H_i$  becomes extremely complicated. The eigenvalues and eigenvectors of  $-H_i$  cannot be expressed analytically, but can only be given numerically. Meanwhile, the Hamiltonian at site  $j$  in the sublattice  $B$  can also be rewritten as

$$H = H_j + H'_j, \quad (6)$$

$$-H_j = E_j S_j^z + D_B (S_j^z)^2 + \Omega S_j^x, \quad (7)$$

and

$$E_j = J \sum_i \sigma_i^z. \quad (8)$$

Within the effective-field theory, the average sublattice magnetizations for the honeycomb lattice are given by<sup>19,20</sup>

$$M_a \equiv \langle \sigma_i^z \rangle = \left[ \cosh(J\eta\nabla) + \frac{M_b}{\eta} \sinh(J\eta\nabla) \right]^3 F_A(x)|_{x=0}, \quad (9)$$

$$\begin{aligned} M_b \equiv \langle S_j^z \rangle &= [q \cosh(J\nabla) + M_a \sinh(J\nabla) + 1 - q]^3 \\ &\quad \times F_B(x)|_{x=0}, \end{aligned} \quad (10)$$

where  $\nabla = \partial/\partial x$  is the differential operator, and  $q$  and  $\eta$  are

$$q \equiv \langle (\sigma_i^z)^2 \rangle = \left[ \cosh(\eta J\nabla) + \frac{M_b}{\eta} \sinh(\eta J\nabla) \right]^3 G_A(x)|_{x=0}, \quad (11)$$

$$\begin{aligned} \eta^2 \equiv \langle (S_j^z)^2 \rangle &= [q \cosh(J\nabla) + M_a \sinh(J\nabla) + 1 - q]^3 \\ &\quad \times G_B(x)|_{x=0}. \end{aligned} \quad (12)$$

The four functions  $F_A(x)$ ,  $F_B(x)$ ,  $G_A(x)$ , and  $G_B(x)$  are defined as

$$F_A(x) = \frac{1}{\sum_{m=1}^3 \exp(\beta\lambda_m)} \left\{ \sum_{m=1}^3 \langle \phi_m | \sigma_i^z | \phi_m \rangle \exp(\beta\lambda_m) \right\}, \quad (13)$$

$$F_B(x) = \frac{1}{\sum_{n=1}^4 \exp(\beta\lambda_n)} \left\{ \sum_{n=1}^4 \langle \varphi_n | S_j^z | \varphi_n \rangle \exp(\beta\lambda_n) \right\}, \quad (14)$$

$$G_A(x) = \frac{1}{\sum_{m=1}^3 \exp(\beta\lambda_m)} \left\{ \sum_{m=1}^3 \langle \phi_m | (\sigma_i^z)^2 | \phi_m \rangle \exp(\beta\lambda_m) \right\}, \quad (15)$$

$$G_B(x) = \frac{1}{\sum_{n=1}^4 \exp(\beta\lambda_n)} \left\{ \sum_{n=1}^4 \langle \varphi_n | (S_j^z)^2 | \varphi_n \rangle \exp(\beta\lambda_n) \right\}, \quad (16)$$

Here, when  $E_i$  (or  $E_j$ ) is replaced by  $x$ ,  $\lambda_m$ , and  $\lambda_n$  in Eqs. (13)–(16) are eigenvalues of  $-H_i$  and  $-H_j$ , respectively.  $\phi_m$  and  $\varphi_n$  are eigenfunctions of  $-H_i$  and  $-H_j$ , respectively. It can be easily proved that functions  $F_A(x)$  and  $F_B(x)$  are odd functions, and  $G_A(x)$  and  $G_B(x)$  are even functions.

We use the fact that even functions of  $\nabla$  must be zero when operating to the odd function.<sup>19–21</sup> In this way, Eqs. (9)–(12) can be rewritten as

$$M_a = A_1(\eta) M_b + A_2(\eta) M_b^3, \quad (17)$$

$$M_b = B_1(q) M_a + B_2(q) M_a^3, \quad (18)$$

$$q = C_1(\eta) + C_2(\eta) M_b^2, \quad (19)$$

$$\eta^2 = D_1(q) + D_2(q) M_a^2. \quad (20)$$

The coefficients  $A_i(\eta)$ ,  $B_i(q)$ ,  $C_i(\eta)$ , and  $D_i(q)$  ( $i=1,2$ ) can be easily calculated by applying a mathematical relation  $e^{\alpha \nabla} f(x) = f(x + \alpha)$  as given in the Appendix.

Then the average total magnetization per site is given by

$$M = (M_a + M_b)/2. \quad (21)$$

The sublattice magnetization  $M_a$  in the vicinity of transition point can be written as

$$M_a^2 = (1-a)/b. \quad (22)$$

The parameters  $a$  and  $b$  are obtained as follows:

$$a = A_1 B_1, \quad (23)$$

$$b = B_1 A_2 + B_2 A_1^3 + \frac{(2\eta_0 A_1 B_1' + B_1 A_1' D_1') C_2}{2\eta_0 - C_1' D_1'} + \frac{(B_1 A_1' A_1^2 + A_1^3 B_1' C_1') D_2}{2\eta_0 - C_1' D_1'}, \quad (24)$$

The coefficients  $A_i$  and  $C_i$  ( $B_i$  and  $D_i$ ,  $i=1,2$ ) are defined as a function of  $\eta_0$  ( $q_0$ ) [ $q_0 = C_1(\eta_0)$ ,  $\eta_0^2 = D_1(q_0)$ ],  $A_1'$  and  $C_1'$  ( $B_1'$  and  $D_1'$ ) denote the first derivative of  $A_1$  and  $C_1$  ( $B_1$  and  $D_1$ ) with  $\eta_0$  ( $q_0$ ). When  $a=1$  and  $b<0$  the transition is the second order; when  $a=1$  and  $b>0$  the transition is the first order; and the tricritical point at which the phase transition changes from the second order to the first order is determined by  $a=1$  and  $b=0$ .<sup>21-25</sup> Further, it should also be noticed that the coefficients  $a$  and  $b$  are even functions of  $J$ . The physical consequence of this fact is that the critical behaviors are the same for the ferromagnetic ( $J>0$ ) or ferrimagnetic ( $J<0$ ) ground state. However, in the ferrimagnetic case, the signs of two sublattice magnetizations are different.

### III. NUMERICAL RESULTS AND DISCUSSIONS

In this section, we show some typical results for the mixed spin-1 and spin- $\frac{3}{2}$  transverse Ising model with different crystal fields for the honeycomb lattice in the ground state. The phase diagrams of the systems can be determined by solving the two conditions ( $a=1$  and  $b<0$  for the second order transition,  $a=1$  and  $b=0$  for the tricritical point) numerically. In order to determine the first-order transition, one usually needs to calculate the free energy for two phases and to find a point of intersection. However, it is true that the first-order transition line is determined by  $a=1$  and  $b>0$ , which is similar to the criterion of the Landau phase transition theory. The application of this method can be found in the literature.<sup>21,23-25</sup> In Refs. 24 and 25 the general expressions for evaluating the second-order phase transition and the tricritical point are obtained by the use of effective-field theory with correlations. Their result for the tricritical point at which the system exhibits a first-order phase transition is in quite good agreement with those obtained by using the series expansion methods. In the remainder of this section, we shall represent our results in the following order: first, the ground states, as a function of the parameters; second, the temperature dependence of the magnetization; third, the be-

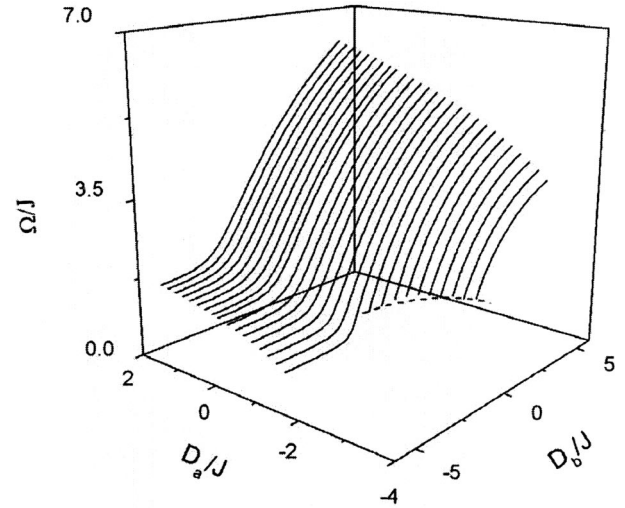


FIG. 1. Phase diagram of the ground states for the system in the parametric ( $\Omega/J$ ,  $D_A/J$ ,  $D_B/J$ ) space. The bold dotted curve represents the positions of tricritical points.

havior of  $T_c$ , as a function of the parameters.

#### A. The ground states

Figure 1 shows the phase diagrams of the ground states of the system in the parametric ( $\Omega/J$ ,  $D_A/J$ ,  $D_B/J$ ) space, where the bold dotted curve is the positions of tricritical points. Each solid curve separates the parametric space into two regions: one is the ferromagnetic (or ferrimagnetic) phase that is located below the phase transition curve, and the other is for the paramagnetic phase above the phase transition curve. From numerical results, when  $D_A/J < -1.25$ , the tricritical points do exist in the system. When  $D_A/J > -1.25$  and the value of transverse magnetic field  $\Omega/J < 0.75$ , the system is always in the ferromagnetic (or ferrimagnetic) phase, independent of the crystal field  $D_B$ . Physically, this result comes from the fact that the sublattice  $B$  approaches the  $S_j^z = \pm \frac{1}{2}$  state and the sublattice  $A$  approaches the  $\sigma_i^z = 0$  state, but the total magnetic order of the mixed-spin system does exist.

In Figs. 2(a)–2(c), the sublattice and total magnetization in the ground states are given for the mixed spin-1 and spin- $\frac{3}{2}$  transverse Ising model with different crystal fields. From Figs. 2(a)–2(c), the magnetization  $M_a$  (or  $M_b$ ) of sublattice  $A$  (or  $B$ ) and the total magnetization  $M$  decrease with increasing the transverse  $\Omega/J$  when  $D_B/J$  (or  $D_A/J$ ) is fixed. This interesting effect is attributed to that the quantum fluctuations become stronger when the value of  $\Omega/J$  increases. From Fig. 2(a), we note that for  $D_A/J \rightarrow +\infty$ , the value of sublattice magnetization approaches  $M_a=1$ , while for  $D_A/J \rightarrow -\infty$ , the value of sublattice magnetization approaches  $M_a=0$ . From Fig. 2(b), we can see that for  $D_B/J \rightarrow +\infty$ , the value of sublattice magnetization approaches  $M_b=3/2$ , while for  $D_B/J \rightarrow -\infty$ , the value of sublattice magnetization approaches  $M_b=\frac{1}{2}$  when the value of  $\Omega/J < 0.75$ . From Fig. 2(c), we again find that for  $\Omega/J < 0.75$ , the total magnetization  $M$  does not reduce to zero for any  $D_B/J$ .

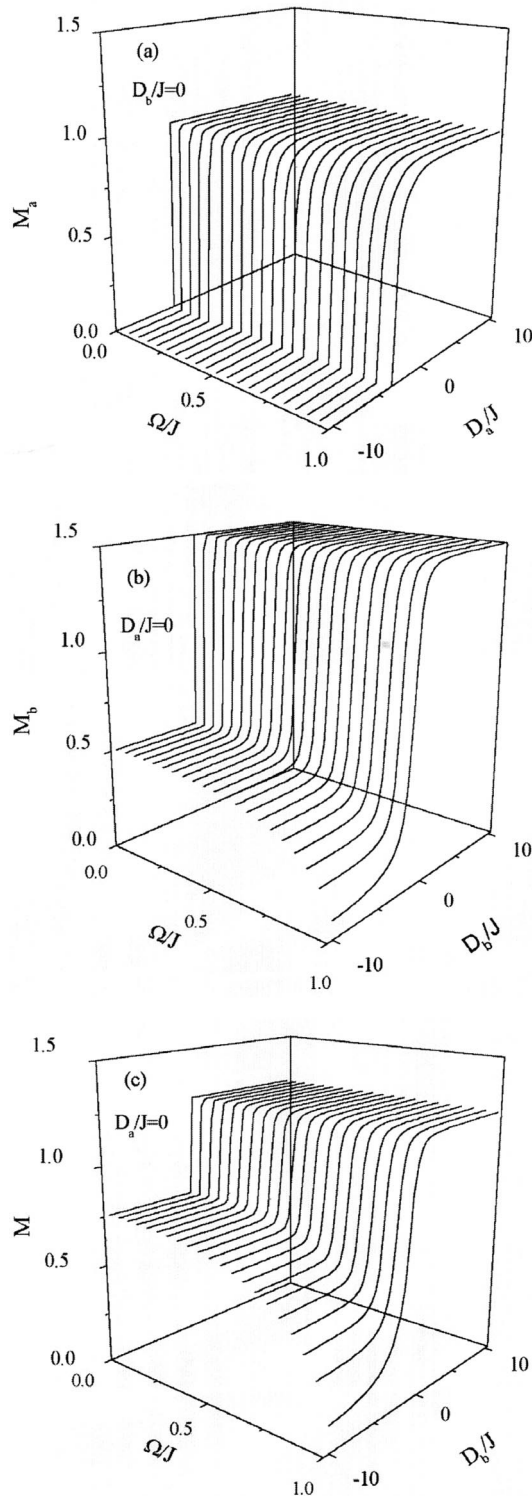


FIG. 2. Magnetization of the ground states for the mixed-spin ferromagnet. (a) In the parametric  $(M_a, \Omega/J, D_A/J)$  space when the value of  $D_B/J=0$ . (b) In the parametric  $(M_b, \Omega/J, D_B/J)$  space when the value of  $D_A/J=0$ . (c) In the parametric  $(M, \Omega/J, D_B/J)$  space when the value of  $D_A/J=0$ .

This is due to the finding that the sublattice  $B$  approaches the  $S_j^z = \pm \frac{1}{2}$  state and the sublattice  $A$  approaches the  $\sigma_i^z = 0$  state, but the total magnetic order of the mixed-spin system

does exist. This result is consistent with the phase diagram of the ground states in Fig. 1.

### B. Temperature dependence of magnetizations

It is known that the role of the crystal fields and transverse field is important for magnetization of the Ising system. The temperature dependence of magnetizations in the mixed spin-1 and spin- $\frac{3}{2}$  system is calculated by solving Eqs. (17)–(20) numerically. Figures 3(a)–3(c) show the temperature dependencies of the sublattices  $(M_a, M_b)$  and total magnetization  $(M)$  with the values of  $\Omega$  and  $D_A$  are fixed at  $\Omega = 0$  and  $D_A/J = -0.5$ , respectively, for mixed-spin ferromagnets. From these figures we can see that all curves except for that labeled by  $D_B/J = -1.5$  correspond to a collinear spin configuration with  $M_a = 1.0$ ,  $M_b = 0.5$  or  $1.5$ ,  $M = 1.25$ , or  $M = 0.75$  at the ground state. The curve labeled by  $D_B/J = -1.5$  corresponds to  $M_a = M_b = M = 0.985$ . It is seen that this result comes from the use of the approximate Van der Waerden identity for the high-spin system.<sup>23</sup> From Figs. 3(b)–3(c), when  $D_B/J \leq -1.6$ , the curves of the  $M_b$  and total magnetization  $M$  have  $P$ -type behavior that usually can be observed only for a ferrimagnet. According to the Néel theory, the shape of the magnetization versus  $T$  curve can exhibit five characteristic features classified as the  $Q$ ,  $P$ ,  $N$ ,  $L$ , and  $M$  types,<sup>26</sup> depending on the direction and magnitude of the respective sublattice magnetizations. A mean-field calculation based on a two-sublattice model also revealed that such ferrimagneticlike behavior could exist for a ferromagnet, due to the competition among the comparatively weak exchange coupling and the opposite sublattice anisotropies.<sup>27</sup> In the present system, the existence of the ferrimagneticlike  $P$ -type curves is ascribed mainly to the competition between the effects of the exchange coupling, the sublattice anisotropies and temperature on the spin configurations in the system. The influence of the transverse field  $\Omega$  can be seen from a comparison between Figs. 3(c) and 3(d). Figure 3(c) shows three fixed values ( $M = 1.25, 0.985$ , and  $0.5$ ) of total magnetization at  $k_B T/J = 0$ , while seven values ( $M = 1.247, 1.244, 1.215, 1.047, 0.932, 0.825$ , and  $0.715$ ) exist at  $k_B T/J = 0$  in Fig. 3(d). The role of the transverse field is to destroy the collinear spin configurations to create more noncollinear spin configurations at the ground state. It is thought that in a certain sense, the temperature has an effect similar to that of the transverse field, so that when the temperature is arisen, the magnetization curve labeled by  $D_B/J = -1.4$  (or  $-1.6$ ) in Fig. 3(d) drops down (or rises up) fast to the value close to the magnetization  $M = 1.047$  (or  $0.825$ ). However, the  $P$ -type ferrimagneticlike curve disappears in Fig. 3(d), since the transverse field alters the spin configurations at the whole temperature range, but the effect of the temperature becomes more pronounced only at intermediate/high temperatures.

The thermal variations of the total magnetization  $|M|$  for the mixed-spin ferrimagnets with  $D_A/J = -0.5$  and  $D_B/J = -1.5$  and  $\Omega/J = 0, 0.05, 0.1, 0.5$  are shown in Fig. 4. The two compensation points exist when the value of transverse field is  $\Omega/J = 0.05$ . In an  $N$ -type ferrimagnet, there is the existence of a finite compensation temperature at which the total magnetization vanishes below the transition tempera-

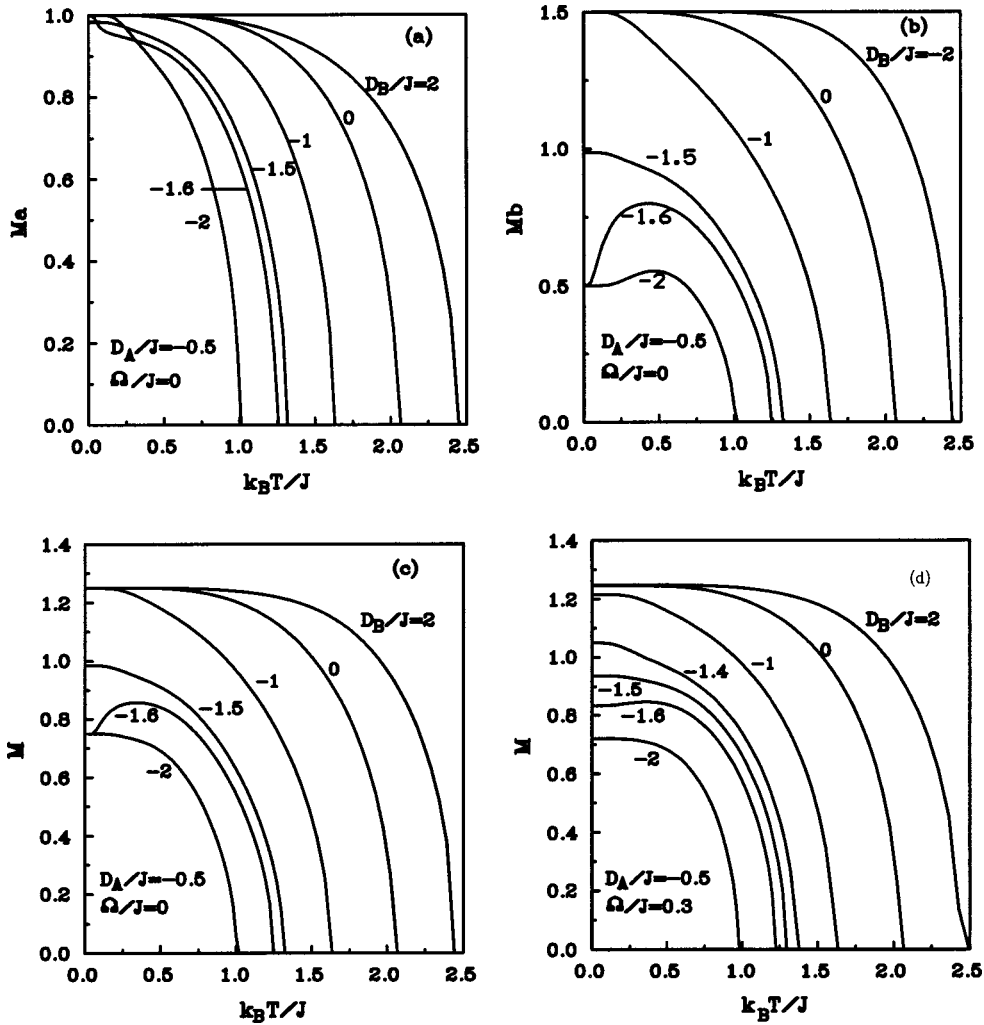


FIG. 3. Temperature dependence of the magnetization for the mixed-spin ferromagnet when the values of  $D_A$  and  $\Omega/J$  are fixed at  $D_A/J = -0.5$  and  $\Omega/J = 0$ , respectively. (a) In the  $(M_a, k_B T/J)$  plane. (b) In the  $(M_b, k_B T/J)$  plane. (c) In the  $(M, k_B T/J)$  plane. (d) In the  $(M, k_B T/J)$  plane when the values of  $D_A$  and  $\Omega/J$  are fixed at  $D_A/J = -0.5$  and  $\Omega/J = 0.3$ , respectively. The numbers at the curves are the values of  $D_B/J$ .

ture. As far as we know, it is noted in the standard textbooks on magnetism<sup>28</sup> that only one compensation point may exist in a ferrimagnetic material. However, very recently, Ohkoshi *et al.*<sup>29</sup> reported that the molecular based ferrimagnets  $((\text{Ni}_a^{\text{II}}\text{Mn}_b^{\text{II}}\text{Fe}_c^{\text{II}})_{1.5}[\text{Cr}^{\text{III}}(\text{CN})_6] \cdot 7.6\text{H}_2\text{O} (a+b+c=1))$  show two compensation points. Kaneyoshi also discussed extensively the possibility of two compensation points in ferrimagnets including the molecular-based magnets.<sup>30</sup> Our calculation results show that two compensation points could possibly occur indeed in the ferrimagnetic materials, depending on the competition among the exchange coupling, the anisotropies, and the transverse field and also on the magnetization of the sublattices.

C. Transition temperatures

In this section, we show results for the phase diagrams of the present systems. Figures 5(a) and 5(b) give the phase diagram for the system in the parametric  $(k_B T_c/J, D_A/J, D_B/J)$  space, when the value of the transverse field is selected as  $\Omega/J = 0.1$  and  $\Omega/J = 0.3$ , respectively. The solid

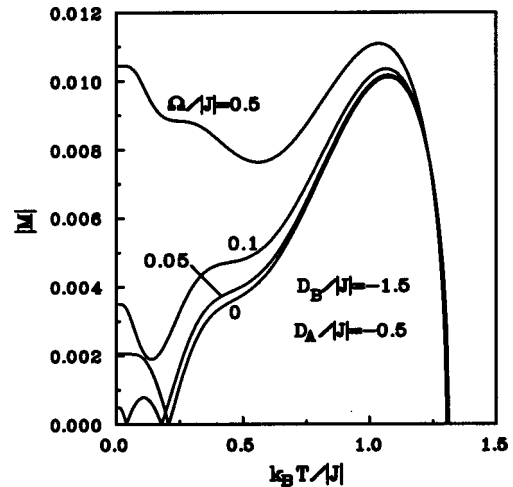


FIG. 4. Temperature dependence of the magnetization  $|M|$  for the mixed-spin ferrimagnet, when the values of  $D_A/|J|$  and  $D_B/|J|$  are fixed at  $D_A/|J| = -0.5$  and  $D_B/|J| = -1.5$ . The numbers at the curves are the values of  $\Omega/|J|$ .

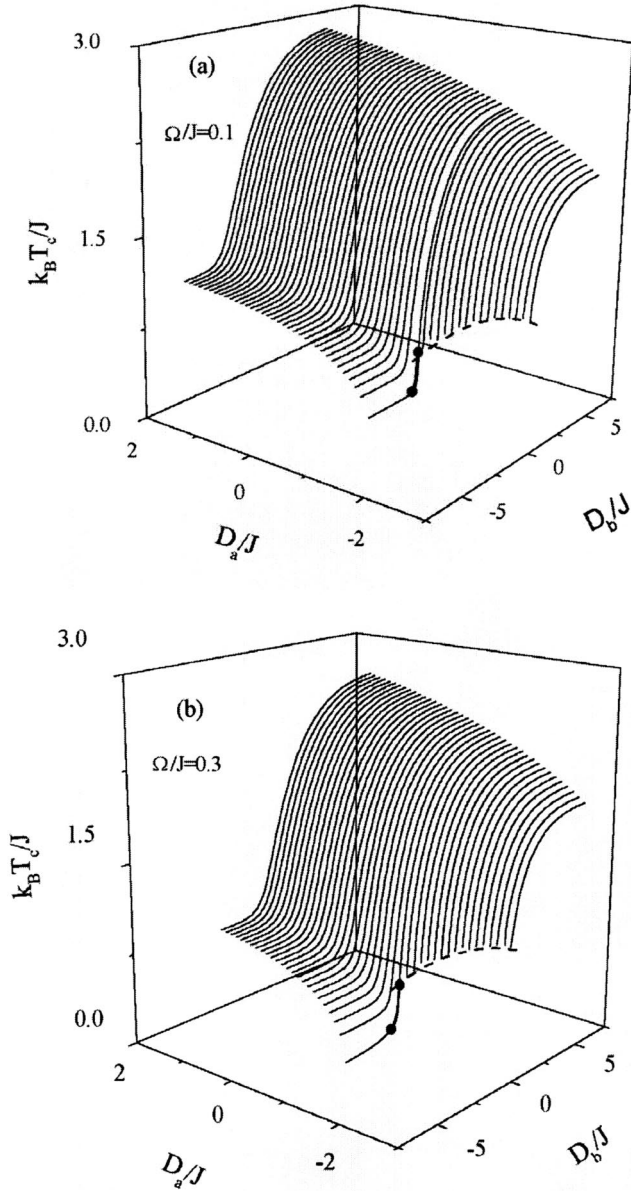


FIG. 5. Phase diagram for the system in the parametric ( $k_B T_c/J$ ,  $D_A/J$ ,  $D_B/J$ ) space. (a) as the transverse field  $\Omega/J = 0.1$ . (b) As the transverse field  $\Omega/J = 0.3$ . The solid circles and dotted curve represent the positions of tricritical points. The light and bold curves are the second-order and first-order phase transition lines, respectively.

circles and dotted curve represent the positions of tricritical points. The light and bold curves are the second-order and first-order phase transition lines, respectively. These two figures clearly illustrate how the transition temperature changes with the values of the crystal fields and the transverse field. At a certain value of the crystal fields, the transverse field makes the transition temperature decrease. The results also indicate that applying the transverse magnetic field can control the transition temperatures and the tricritical points of the system. From our calculation, we note that for  $D_B/J \rightarrow +\infty$  when the spin  $\frac{3}{2}$  behaves like a two-level system with

$S_j^z = \pm \frac{3}{2}$ , there is no tricritical point on the phase diagrams. In the other limit, for  $D_B/J \rightarrow -\infty$ , the  $S_j^z = \pm \frac{3}{2}$  states are suppressed and the system becomes equivalent to a mixed spin- $\frac{1}{2}$  and spin-1 Ising model. At  $D_A/J = 0$ , the transition temperature is  $k_B T_c/J = 0.891$  and no tricritical point exists for this situation, which is the same as the result given in Ref. 8. In particular, the value of the transition temperature in the absence of the crystal fields ( $D_A/J = D_B/J = 0$ ) is  $k_B T_c/J = 2.119$  at the transverse field  $\Omega/J = 0.1$ . From Fig. 5(a), we also know that when the value of  $D_B/J$  ( $D_A/J$ ) satisfies  $D_B/J \leq -2.1$  or  $D_B/J \geq 0.79$  ( $D_A/J \geq -1.37$ ) while the values of  $D_A/J$  ( $D_B/J$ ) vary in the system, no tricritical point exists. Namely, only the second-order magnetic phase transition exists. When  $-2.1 < D_B/J < 0.79$ , the tricritical point appears at the transverse field  $\Omega/J = 0.1$ , where both the first- and the second-order phase transitions coexist. In the region  $-1.639 < D_B/J < -1.627$  (or  $-1.49 < D_A/J < -1.42$ ), two tricritical points exist when the values of  $D_A/J$  (or  $D_B/J$ ) vary in the system.

Where a second-order phase line meets a first-order phase boundary, a tricritical point occurs. The occurrence of the multicritical points depends on the values of  $D_A/J$  and  $D_B/J$ . For  $-1.639 < D_B/J < -1.627$  and  $-1.49 < D_A/J < -1.42$ , the spin configuration of the system at the ground state should be the following situation: most of the  $\sigma_i^z$  spins are in the  $\sigma_i^z = 0$  state and the remainder are randomly occupied by  $\sigma_i^z = \pm 1$ , while all  $S_j^z$  spins are randomly occupied by  $S_j^z = \pm \frac{3}{2}$  states because the lower-energy state is favored. In this case, the effect of the sublattice magnetization  $A$  is very weak because most of  $\sigma_i^z$  spins are in the  $\sigma_i^z = 0$  state. The system behaves like the spin- $\frac{3}{2}$  Blume-Capel model,<sup>31</sup> since when the transverse field is absent, i.e.,  $\Omega/J = 0$ , the present model could be reduced to the Blume-Capel model. The sublattice magnetization  $B$  does exist ( $M_B \neq 0$ ); thus the total magnetization is not zero ( $M \neq 0$ ) at zero temperature. When the temperature increases from zero, some of the  $\sigma_i^z$  spins in the  $\sigma_i^z = 0$  state can suddenly occupy the  $\sigma_i^z = +1$  (or  $\sigma_i^z = -1$ ) state, while half of the spins take the  $S_j^z = +\frac{3}{2}$  (or  $S_j^z = -\frac{3}{2}$ ) state and others take  $S_j^z = -\frac{1}{2}$  (or  $S_j^z = +\frac{1}{2}$ ). The effects of the occupations in the states of the spins could lead to vanishing of the total magnetization ( $M = 0$ ) at a certain temperature, resulting in the occurrence of the first-order phase transition.<sup>20</sup> The discussion above explains why the first tricritical point (solid circle) occurs. With increasing the value of crystal fields, most of the spins  $S_j^z$  are in the  $S_j^z = \pm \frac{3}{2}$  state, so the total magnetization appears ( $M \neq 0$ ) again on the curve, namely, the additional tricritical point (solid circle) appears in the system with appropriate negative values of  $D_A/J$  and  $D_B/J$  on the curve. The first tricritical point probably comes from the fact that the spin- $\frac{3}{2}$  Blume-Capel model exhibits an unstable first-order transition, and the second tricritical point has its origin in the spin-1 Blume-Capel model.<sup>32</sup> In Fig. 5(b), we also find from the numerical calculation that when the transverse field increases ( $\Omega/J = 0.3$ ), the phenomena of the existence of two tricritical points disappear on the curve. It is concluded that within the

framework of the effective-field theory with correlations, two tricritical points could be detected in the mixed spin-1 and spin- $\frac{3}{2}$  Ising system on a honeycomb lattice, which result from different anisotropies. From the previous work,<sup>17,32</sup> one of the two tricritical points is stable, whereas another is unstable. For the difference between the unstable and stable tricritical points, readers should refer to the detailed investigations on this topic in Refs. 17 and 32. When the value of  $D_B/J$  ( $D_A/J$ ) satisfies  $D_B/J \leq -2.3$  or  $D_B/J \geq 0.82$  ( $D_A/J \geq -1.37$ ) while the values of  $D_A/J$  ( $D_B/J$ ) varies in the system, no tricritical point exists. Namely, only the second-order magnetic phase transition exists. When  $-2.3 < D_B/J < 0.82$ , the tricritical point appears at the transverse field  $\Omega/J=0.3$ , where both the first- and the second-order phase transitions coexist.

For the accuracy of the EFT and the limitations of the method, we think that the accuracy of the EFT must be better than the normal mean-field theory. The EFT is still within the framework of the mean-field theory. The mean-field theory usually gives incorrect results of the critical exponents when one studies the critical behaviors at the critical points. However, it is a fact that the mean-field theory is good enough to give the exact values for the critical points, the magnetization far from the critical points, etc. In the present work, we do not investigate the critical exponents. Thus the problems of the accuracy of the EFT and the limitations of the method do not affect the correctness of the results of the present work.

#### IV. CONCLUSIONS

In this work, we have studied the phase diagrams and magnetizations of the mixed spin-1 and spin- $\frac{3}{2}$  transverse Ising model with the presence of the crystal fields on the honeycomb lattice by the use of the effective-field theory. We have examined the critical properties of the system numerically by solving the equations given in Sec. II. The transition temperature determined from Eqs. (23) and (24) is independent of the sign of  $J$  and thus the relation is valid for both ferromagnetic ( $J>0$ ) and ferrimagnetic ( $J<0$ ) cases. The magnetic properties of the ground states for the system have been studied. We have also discussed in detail the influence of the transverse field and the crystal fields on the transition temperatures and magnetizations. A number of interesting phenomena, originating from the competition between the transverse field and the crystal field, have been found. The system can exhibit two tricritical points when the anisotropy of one of the sublattices is varied at fixed values of the anisotropy of another sublattice and transverse field. The mixed-spin ferromagnetic system with the presence of the transverse and crystal fields can show a  $P$ -type ferrimagneticlike temperature dependence of magnetization, which exists usually only in a ferrimagnet. The mixed-spin ferrimagnetic system with the presence of the transverse and crystal fields can exhibit two compensation points, which is

not predicted in the Néel theory of ferrimagnetism. However, these results are obtained within the framework of the EFT. It is necessary to indicate that these results must be subjected to further tests by more adequate techniques such as Monte Carlo numerical simulations or renormalization techniques.

On the other hand, according to the EFT, the Hamiltonian can be separated into two parts ( $H=H_{i(j)}+H'_{i(j)}$ ). One ( $H_{i(j)}$ ) includes all parts of  $H$  associated with the site  $i$  ( $j$ ), which do not commute with  $H$ , so the eigenvalues of  $-H_{i(j)}$  cannot be given analytically, but can only be given numerically. This method can also be extended for studying other more complicated mixed transverse Ising mode with crystal fields.

#### ACKNOWLEDGMENTS

The National Natural Sciences Foundation of China has supported this work under Grants No. 59725103 and No. 10274087.

#### APPENDIX

We have

$$A_1 = \frac{3}{4\eta} [F_A(3J\eta) + F_A(J\eta)],$$

$$A_2 = \frac{1}{4\eta^3} [F_A(3J\eta) - 3F_A(J\eta)],$$

$$B_1 = 3 \left\{ \frac{q^2}{4} [F_B(3J) + F_B(J)] + q(1-q)F_B(2J) + (1-q)F_B(J) \right\},$$

$$B_2 = \frac{1}{4} [F_B(3J) - 3F_B(J)],$$

$$C_1 = \frac{1}{4} [G_A(3\eta J) + 3G_A(\eta J)],$$

$$C_2 = \frac{3}{4\eta^2} [G_A(3\eta J) - G_A(\eta J)]$$

$$D_1 = \frac{q^3}{4} [G_B(3J) + 3G_B(J)] + \frac{3}{2} q^2(1-q)[G_B(2J) + G_B(0)] + 3q(1-q)^2 G_B(J) + (1-q)^3 G_B(0),$$

$$D_2 = \frac{3q}{4} [G_B(3J) - G_B(J)] + \frac{3}{2} (1-q)[G_B(2J) - G_B(0)].$$

- \*Corresponding author. Email address: wjiang@imr.ac.cn
- <sup>1</sup>C. Mathoniere, C. J. Nuttall, S. G. Carlin, and P. Day, *Inorg. Chem.* **351**, 201 (1996).
- <sup>2</sup>Proceedings of the Conference On Ferromagnetic and High Spin Molecular-Based Materials, edited by H. Iwamura and J. S. Miller, *Mol. Cryst. Liq. Cryst.* **232** (1993).
- <sup>3</sup>J. Manriquez, G. T. Lee, R. Scott, A. Epstein, and J. Miller, *Science* **252**, 1415 (1991).
- <sup>4</sup>M. Jaščur and S. Lacková, *J. Phys.: Condens. Matter* **12**, L583 (2000).
- <sup>5</sup>G. M. Buendia and J. A. Liendo, *J. Phys.: Condens. Matter* **9**, 5439 (1997).
- <sup>6</sup>G. M. Buendia and M. A. Novotny, *J. Phys.: Condens. Matter* **9**, 5951 (1997).
- <sup>7</sup>G. M. Buendía and R. Cardona, *Phys. Rev. B* **59**, 6784 (1999).
- <sup>8</sup>T. Kaneyoshi, *J. Phys. Soc. Jpn.* **56**, 2675 (1987).
- <sup>9</sup>A. Bobák and M. Jaščur, *Phys. Rev. B* **51**, 11533 (1995).
- <sup>10</sup>S. L. Yan and C. Z. Yang, *Phys. Rev. B* **57**, 3512 (1998).
- <sup>11</sup>T. Kaneyoshi, *Z. Phys. B: Condens. Matter* **71**, 109 (1988).
- <sup>12</sup>A. Bobák and D. Horváth, *Phys. Status Solidi B* **213**, 459 (1999).
- <sup>13</sup>R. G. Bowers and B. Y. Yousif, *Phys. Lett. A* **96**, 49 (1983).
- <sup>14</sup>G. J. A. Hunter, R. C. L. Jenkines, and C. J. Tinsley, *J. Phys. A* **23**, 4547 (1990).
- <sup>15</sup>X. M. Weng and Z. Y. Li, *Phys. Rev. B* **53**, 12142 (1996).
- <sup>16</sup>S. G. A. Quadros and S. R. Salinas, *Physica A* **206**, 479 (1994).
- <sup>17</sup>A. Bobák, *Physica A* **286**, 531 (2000); **258**, 140 (1998).
- <sup>18</sup>O. F. Abubrig, D. Horváth, A. Bobák, and M. Jaščur, *Physica A* **296**, 437 (2001).
- <sup>19</sup>W. Jiang, G. Z. Wei, and Z. H. Xin, *Physica A* **293**, 455 (2001).
- <sup>20</sup>G. Z. Wei, Z. H. Xin, and J. Wei, *J. Magn. Magn. Mater.* **204**, 144 (1999).
- <sup>21</sup>T. Kaneyoshi, *Acta Phys. Pol. A* **83**, 703 (1993).
- <sup>22</sup>F. C. Sá. Barreto, I. P. Fittipaldi, and B. Zerks, *Ferroelectrics* **39**, 1103 (1981); F. C. Sá. Barreto and I. P. Fittipaldi, *Physica A* **129**, 360 (1985).
- <sup>23</sup>T. Kaneyoshi, J. W. Tucker, and M. Jaščur, *Physica A* **186**, 495 (1992).
- <sup>24</sup>T. Kaneyoshi, *J. Phys. C* **19**, L557 (1986).
- <sup>25</sup>A. F. Siqueira and I. P. Fittipaldi, *Physica A* **138**, 592 (1986).
- <sup>26</sup>M. L. Néel, *Ann. Phys. (Paris)* **3**, 137 (1948).
- <sup>27</sup>Z. D. Zhang, M. H. Yu, and T. Zhao, *J. Magn. Magn. Mater.* **174**, 261 (1997).
- <sup>28</sup>S. V. Tyabrikov, *Methods in Quantum Theory of Magnetism* (Plenum, New York, 1967).
- <sup>29</sup>S. Ohkoshi, Y. Abe, A. Fujishima, and K. Hashimoto, *Phys. Rev. Lett.* **82**, 1285 (1999).
- <sup>30</sup>T. Kaneyoshi, *J. Phys. Soc. Jpn.* **70**, 884 (2001).
- <sup>31</sup>M. Blume, *Phys. Rev.* **141**, 517 (1966); H. W. Capel, *Physica (Amsterdam)* **32**, 966 (1966).
- <sup>32</sup>T. Kaneyoshi and M. Jaščur, *Physica B* **179**, 317 (1992).